Modeling and Visualization of Receptor Clustering on the Cellular Membrane

Martin Falk* Markus Daub† Guido Schneider† Thomas Ertl*

* VISUS – Visualization Research Center, University of Stuttgart, Germany
† Institute of Analysis, Dynamics, and Modeling, University of Stuttgart, Germany

ABSTRACT

In cell biology, apopotosis is a very important cellular process. Apopotosis, or programmed cell death, allows an organism to remove damaged or unneeded cells in a structured manner in contrast to necrosis. Ligands bind to the death receptors located on the cellular membrane forming ligand-receptor clusters.

In this paper, we develop a novel mathematical model describing the stochastic process of the ligand-receptor clustering. To study the structure and the size of the ligand-receptor clusters, a stochastic particle simulation is employed. Besides the translation of the particles on the cellular membrane, we also take the particle rotation into account as we model binding sites explicitly. Glyph-based visualization techniques are used to validate and analyze the results of our *in-silico* model. Information on the individual clusters as well as particle-specific data can be selected by the user and is mapped to colors to highlight certain properties of the data.

The results of our model look very promising. The visualization supports the process of model development by visual data analysis including the identification of cluster components as well as the illustration of particle trajectories.

Index Terms: I.3.3 [Computer Graphics]: Picture/Image Generation; I.3.7 [Computer Graphics]: Three-Dimensional Graphics and Realism; I.3.8 [Computer Graphics]: Applications; I.6.5 [Simulation and Modeling]: Model Development—Modeling Methodologies; I.6.8 [Simulation and Modeling]: Types of Simulation—Discrete Event; J.3 [Life and Medical Sciences]: Biology and Genetics;

1 INTRODUCTION

Apoptosis is a significant physiological process since it enables the organism to remove unwanted or damaged cells. The molecular mechanism of the apoptotic process is very complex so that the underlying network is difficult to understand in detail. However, two major pathways can be distinguished: the extrinsic and the intrinsic signaling pathway. In this article, we focus on the extrinsic pro-apoptotic signaling pathway. The external stimulus of the extrinsic pathway is the clustering of death receptors on the cell membrane: signal competent ligand-receptor clusters activate caspases, a special type of proteins, upon cleavage and thereby stimulate the caspase cascade.

Our model is concerned with the dynamics of these ligand-receptor clusters. Subjects to research are how clusters are built, are clusters stable, and what are the dynamics of clusters. The diffusion process of the death receptors and the corresponding death receptor ligands is modeled by a Langevin equation. Coupling the diffusion with particle rotation and particle-particle interactions results in a system of nonlinearly coupled stochastic differential equations.

*e-mail: {falk|ertl}@vis.uni-stuttgart.de
†e-mail: {daub|schneider}@mathematik.uni-stuttgart.de

IEEE Symposium on Biological Data Visualization
October 23 - 24, Providence, Rhode Island, USA
978-1-4673-0004-9/11/$26.00 ©2011 IEEE

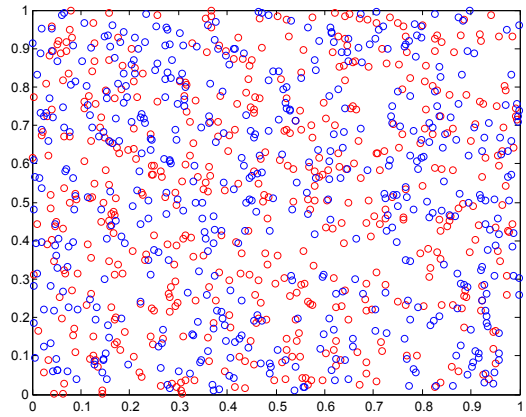

Figure 1: The classical visualization in Matlab gives an overview on the locations of receptors (red) and ligands (blue). Connections between particles and unbound binding sites are missing.

Solving these equations with a particle-based simulation allows us to study the development of ligand-receptor clusters on a planar domain.

In Figure 1, a classical Matlab visualization of ligand-receptor clustering data is depicted. The locations of receptors and ligands can be seen in the overview but no information is given on protein interactions or clusters. Clusters can only be guessed by considering proteins which are close to each other. To be able identifying clusters, all available information contained in the data should be used and be presented in a meaningful way.

The visualization we present uses glyphs for rendering receptors and ligands. By including the binding sites, it is possible to indicate occupied and free bindings sites as well as the orientation and interactions in detailed views. We use different coloring modes for the proteins, i.e. receptors and ligands, depending on the state of each protein or on information of the cluster containing the protein. To deal with the different scales of the data, i.e. simulation domain, protein level, and below, dynamic, distance dependent scaling is used and parts of the visualization can be layered on top of each other to reduce occlusion. Combined with protein trajectories over multiple time steps, this visualization is a powerful tool to ease model development of the ligand-receptor clustering model and to get a deeper insight into the data.

The major contributions of this paper are

- mathematical model for ligand-receptor clustering
- simulation of ligand-receptor clustering
- glyph-based visualization for cluster analysis

The remainder of this paper is structured as follows. Related Work is covered in Section 2. The biological background on apoptosis is given in Section 3. The mathematical model is elaborated

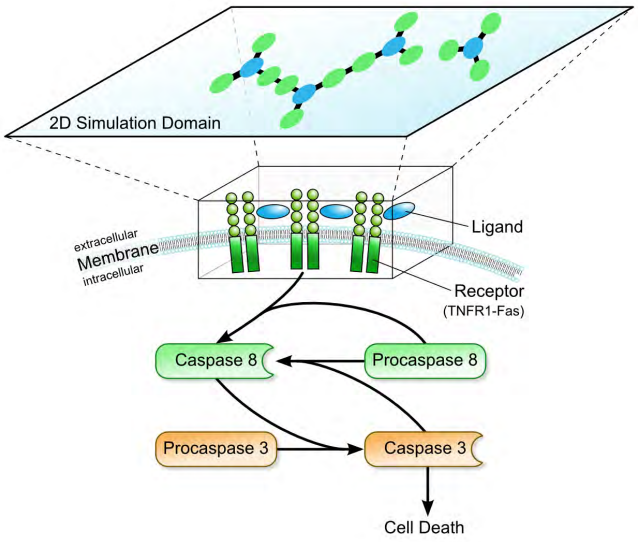

Figure 2: Extrinsic pro-apoptotic signaling pathway. Ligands bind to receptors (TNFR1-Fas) on the cellular membrane, which in turn triggers the signaling pathway. A section of the membrane describes the domain of our ligand-receptor clustering model.

in Section 4. Section 5 details the simulation and the used parameters. In Section 6, our glyph-based visualization approach is explained. Results including statements of a domain expert are given in Section 7. Finally, Section 8 summarizes the paper and gives an outlook.

2 Related Work

Several mathematical models of ligand-receptor clustering on cell surfaces have been established in recent years. In [11], Perelson and DeLisi introduced a model for the cluster formation kinetics. In this model, mass action kinetics for the receptor and ligand concentrations resulted in a system of coupled nonlinear differential equations whose solution describes the cluster size distribution as a function of time. In [6], Guo and Levine introduced a thermodynamic model of ligand-receptor clustering which includes the spatial extension of the cell membrane. Besides, Guo and Levine dealt with a special type of receptors and ligands, namely TNF receptor 1 and the corresponding TNF ligands. In this model, the cell surface is treated as a lattice and the receptor molecules are associated with the lattice site. We seize the idea of the spatial extension of the cell surface and introduce a model where the particles perform a lattice free motion on the cell membrane according to a Brownian motion. Besides the translation of the particles, we take into account the orientation of the particles and consider a Brownian motion for the particle rotation. Our model allows the determination of the size and the structure of the ligand-receptor clusters and can easily be transferred to other receptor and ligand structures.

Glyph-based rendering performed on the graphics processing unit (GPU) allows interactive display of tens or hundreds of thousands objects. Gumhold [5] uses implicitly-described ellipsoids for the visualization of symmetric tensor fields. The surface of the ellipsoids is obtained by ray casting in the fragment shader. Klein and Ertl proposed a similar approach while reducing the necessary information transferred to the GPU [8]. The glyph-based approach was later refined [12] to render dipoles consisting of spherical and cylindrical implicit surfaces. The geometry shader provided by recent GPUs can be used to generate a tighter silhouette geometry as input for the ray casting instead of quadrilateral point splats [3]. Ellipsoids are used by Grottel et al. [4] to represent clusters in data

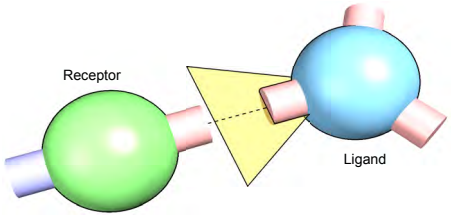

Figure 3: Glyph representations of a TNFR1-Fas receptor (left) and a TNF ligand (right). A receptor has two binding sites. One for a receptor, the second one to connect to a ligand. Ligands have three binding sites for receptors. The possible angular sector for a proper connection of one ligand binding site is depicted in yellow.

from molecular thermodynamics simulations. To match the appearance of particle clusters more closely, GPU-based metaballs [10] can be employed. However, in this work we are not interested in a special cluster representation but want to focus on the internal structure of the clusters instead.

3 Biological Background

The central and executing machinery of apoptosis is the caspase cascade, a network of specific proteases, the caspases. Proteases are proteins which are able to cleave and thereby activate other proteins. In the following, we focus on the extrinsic pro-apoptotic signaling pathway (cf. Figure 2), one of the two signaling pathways which converge at the level of caspase cascade. Two types of caspases are involved in the main part of the reaction network of the extrinsic signaling pathway: the initiator caspase 8 and the effector caspase 3. Both caspase types exist in cells as proenzymes where the inactive form of caspase 8 gets activated through cleavage for example at death receptor complexes. The main part of the reaction network is the activation of pro-caspase 8 by caspase 3 and the activation of pro-caspase 3 by caspase 8. Finally, caspase 3 cleaves several proteins in the cell and thereby dismantles the cell.

The external stimulus of the extrinsic pro-apoptotic signaling pathway is the activation of pro-caspase 8 at the signal competent ligand-receptor clusters. These clusters on the cell membrane consist of death receptors and the corresponding death receptor ligands. The ligand under consideration is the Tumor Necrosis Factor (TNF) ligand and the receptor belongs to the TNF receptor superfamily, e.g. TNF receptor of type 1 (TNFR1). Here, we consider a modified TNFR1 which consists of the extracellular domains of TNFR1 and the cytoplasmic part of the Fas receptor, a so called TNFR1-Fas chimera [1]. TNF exists as a homotrimer which is able to bind three TNF receptors. The TNFR1-Fas receptor contains four extracellular cysteine rich domains (CRD) of which the membrane distal part CRD1 enables the multimerization of TNFR1-Fas receptors [1]. The association of TNF ligands and TNFR1-Fas receptors occurs via the domains CRD2 and CRD3.

4 Model

For the mathematical model of the ligand-receptor clustering, we assume that the TNF ligand possesses three binding sites for the association with TNFR1-Fas receptors according to the homotrimeric structure. Furthermore, TNFR1-Fas receptors have two binding sites, one for a TNF ligand and another for the association with TNFR1-Fas receptors. Therefore, TNFR1-Fas receptors are modeled by a disc with two sectors and the TNF ligands accordingly by a disc with three sectors where the sectors correspond to the binding sites of the particles (see Figure 3). The underlying domain of our two-dimensional model is a unit square with periodic boundary conditions representing a section of the cellular membrane.

Since the motion of the TNF ligands and TNFR1-Fas receptors is driven by diffusion, the motion of the particles is modeled by a Langevin equation

$$m\dot{v} = F - \beta v + X_t,$$

where v is the velocity of the particle, m its mass, β the friction coefficient, F the external force given by the gradient of an interaction potential, and X_t is a random force. We assume that X_t is normally distributed with mean zero and variance σ^2, i.e. $X_t \sim \mathcal{N}(0,\sigma^2)$, where $\sigma = \sqrt{2k_BT\beta}$. Here, k_B is Boltzmann's constant and T is the temperature in Kelvin. Furthermore, we assume that the friction force is of Stoke's type so that the coefficient β has the form $\beta = 6\pi\eta R$, where η is the viscosity of the cell membrane and R is the radius of the particle. The value for η is given in [7] and takes the value $\eta \approx 100\,\mathrm{cP} = 0.1\,\frac{\mathrm{Ns}}{\mathrm{m}^2}$. The value for the radius of the particle is estimated to be $R \approx 3\mathrm{nm}$.

We introduce the dimensionless magnitudes $\bar{x} = x/L$, $\bar{t} = t/\tau$, and $\bar{F} = L/\varepsilon \cdot F$, where ε is the binding energy between the particles, τ the time scale, and L the length scale of the cell. We obtain

$$\frac{L}{\tau^2} m\ddot{\bar{v}} = \frac{\varepsilon}{L}\cdot\bar{F} - \beta\frac{L}{\tau}\bar{v} + \sqrt{2k_BT\beta}\cdot\tilde{X}_t \tag{1}$$

with $\tilde{X}_t \sim \mathcal{N}(0,1)$. Since the mass of a TNF homotrimer is about $m_{\mathrm{TNF}} \approx 51\mathrm{kDa} \approx 8.469\cdot 10^{-23}\mathrm{kg}$ and the mass of a TNFR1-Fas receptor is of the same order, the left hand side of (1) is negligible to the right hand side. Then, equation (1) becomes

$$\bar{v} = \frac{\varepsilon\tau}{L^2\beta}\bar{F} + \sqrt{\frac{2k_BT\tau^2}{L^2\beta}}\cdot\tilde{X}_t. \tag{2}$$

The binding energy ε between two TNFR1-Fas receptors can be estimated by the binding energy between two TNF receptors of type 1 which is given by $\varepsilon_{\mathrm{RR}} \approx 6k_BT$. The binding energy of a TNFR1-Fas receptor and a TNF ligand is similarly proposed to be $\varepsilon_{\mathrm{RL}} \approx 60k_BT$, cf. [6]. Thus, we set $\varepsilon = 6k_BT$ and multiply the external force by a factor 10, if the interaction occurs between a TNF ligand and a TNFR1-Fas receptor. With these assumptions, we obtain from (2)

$$\frac{\mathrm{d}\bar{x}}{\mathrm{d}\bar{t}} = \bar{v} = 6\mu^2\bar{F} + \sqrt{2\tau}\mu\tilde{X}_t \tag{3}$$

with $\mu^2 = \frac{k_BT\tau}{L^2\beta}$. The solution of (3) can formally be written as

$$\bar{x}_{\bar{t}} = \bar{x}_0 + \int_0^{\bar{t}} 6\mu^2\bar{F}\,\mathrm{d}\bar{s} + \int_0^{\bar{t}} \sqrt{2\tau}\mu\,\mathrm{d}\tilde{W}_s \tag{4}$$

with $\mathrm{d}\tilde{W}_s = \tilde{X}_s\mathrm{d}\bar{s}$, where the second integral in (4) is an Ito stochastic integral with respect to a Wiener process $W = \{W_t, t \geq 0\}$.

Equation (4) finally can be written as a stochastic differential equation

$$\mathrm{d}\bar{x} = 6\mu^2\bar{F}\mathrm{d}\bar{t} + \sqrt{2\tau}\mu\mathrm{d}\widetilde{W}_t, \tag{5}$$

cf. [9].

The external force $\bar{F}$ for the interaction between two TNFR1-Fas receptors is given by the negative gradient of a Lennard-Jones potential

$$\bar{V}_{\mathrm{LJ}}(\bar{r},\varphi) = \gamma_n\left(\left(\frac{\bar{\sigma}_{\mathrm{LJ}}}{\bar{r}}\right)^{2n} - \alpha_n\left(\frac{\bar{\sigma}_{\mathrm{LJ}}}{\bar{r}}\right)^{n}\cdot\cos(\varphi-\varphi_0)\right)$$

where φ_0 defines the binding site of the TNFR1-Fas receptor for the association with TNFR1-Fas receptors. The minimum of the dimensionless Lennard-Jones potential takes the value -1 and is reached for the distance between two particles of $\bar{r}^* = 2\bar{\sigma}_{\mathrm{LJ}}$. The dimensionless parameter $\bar{\sigma}_{\mathrm{LJ}}$ corresponds to the radius of the particles. The value of the minimum corresponds to the binding energy of $-\varepsilon$ of the physical Lennard-Jones potential. These properties are described by the conditions

$$\frac{\partial\bar{V}}{\partial\bar{r}}(2\bar{\sigma}_{\mathrm{LJ}},\varphi_0) = 0 \quad \text{and} \quad \bar{V}_{\mathrm{LJ}}(2\bar{\sigma}_{\mathrm{LJ}},\varphi_0) = -1 \tag{6}$$

which yield the parameter values $\gamma_n = 2^{2n}$ and $\alpha_n = 2^{1-n}$. For the interaction between a TNF ligand and a TNFR1-Fas receptor, the cosine in the Lennard-Jones potential is replaced by $\cos(3(\varphi-\varphi_0))$ in order to account for the three attractive binding sites of TNF ligands.

Since we consider several TNFR1-Fas receptors and TNF ligands, we get a system of stochastic differential equations which are nonlinearly coupled by the interaction potential

$$\mathrm{d}\bar{x}_{\mathrm{R}_i} = 6\mu^2\bar{F}_{\mathrm{R}}(\bar{x}_{\mathrm{R}_1},\ldots,\bar{x}_{\mathrm{R}_r},\bar{x}_{\mathrm{L}_1},\ldots,\bar{x}_{\mathrm{L}_s})\mathrm{d}\bar{t} + \sqrt{2\tau}\mu\mathrm{d}\widetilde{W}_{\mathrm{trans},t,i}, \tag{7}$$

$$\mathrm{d}\bar{x}_{\mathrm{L}_j} = 6\mu^2\bar{F}_{\mathrm{L}}(\bar{x}_{\mathrm{R}_1},\ldots,\bar{x}_{\mathrm{R}_r},\bar{x}_{\mathrm{L}_1},\ldots,\bar{x}_{\mathrm{L}_s})\mathrm{d}\bar{t} + \sqrt{2\tau}\mu\mathrm{d}\widetilde{W}_{\mathrm{trans},t,j}, \tag{8}$$

$1 \leq i \leq r, 1 \leq j \leq s$, where r and s are the number of TNFR1-Fas receptors and TNF ligands, respectively.

Additionally, the particles perform a rotational movement which is described by the angular velocity ω and the torsion angle ψ, respectively. The particle rotation is also modeled by a Langevin equation

$$I\dot{\omega} = -\gamma_{\mathrm{rot}}\omega - D_{\mathrm{drill}}(\psi) + \sigma_{\mathrm{rot}}\tilde{D}_t,$$

where the forces are replaced by torsional moments and the mass is replaced by the moment of inertia.

Similar considerations yield a system of stochastic differential equations for the torsion angles

$$\mathrm{d}\bar{\psi}_{\mathrm{R}_i} = -\kappa\mu^2\zeta^2\bar{g}_R(\bar{\psi}_{\mathrm{R}_i})\mathrm{d}\bar{t} + \sqrt{2\tau}\mu\zeta\mathrm{d}\widetilde{W}_{\mathrm{rot},t,i}, \tag{9}$$

$$\mathrm{d}\bar{\psi}_{\mathrm{L}_j} = -\kappa\mu^2\zeta^2\bar{g}_L(\bar{\psi}_{\mathrm{L}_j})\mathrm{d}\bar{t} + \sqrt{2\tau}\mu\zeta\mathrm{d}\widetilde{W}_{\mathrm{rot},t,j}, \tag{10}$$

$1 \leq i \leq r, 1 \leq j \leq s$, where we set $D_{\mathrm{drill}}(\bar{\psi}) = D_r\cdot\bar{g}_{L,R}(\bar{\psi}) = \kappa\cdot k_BT\bar{g}_{L,R}(\bar{\psi})$ and ζ is defined by $\zeta^2 = \beta L^2/\,\gamma_{\mathrm{rot}}$. The function $\bar{g}_{L,R}(\bar{\psi})$ contains the dependency of the particle rotation on the orientation of the binding sites related to the orientation of the linked particles and the parameter κ is a proportional constant which will be determined by computer simulations.

5 Simulation

In order to simulate the clustering of TNF ligands and TNFR1-Fas receptors, we solve the system of nonlinearly coupled stochastic differential equations (7) - (10) numerically by using a Euler-Maruyama approximation of the system (7) - (10)

$$\begin{aligned}
\Delta\bar{x}_{\mathrm{R}_i} &= 6\mu^2\bar{F}_{\mathrm{R}}(\bar{x}_{\mathrm{R}_1},\ldots,\bar{x}_{\mathrm{R}_r},\bar{x}_{\mathrm{L}_1},\ldots,\bar{x}_{\mathrm{L}_s})\Delta\bar{t} + \sqrt{2\tau}\mu\Delta\widetilde{W}_{\mathrm{trans},t,i},\\
\Delta\bar{x}_{\mathrm{L}_j} &= 6\mu^2\bar{F}_{\mathrm{L}}(\bar{x}_{\mathrm{R}_1},\ldots,\bar{x}_{\mathrm{R}_r},\bar{x}_{\mathrm{L}_1},\ldots,\bar{x}_{\mathrm{L}_s})\Delta\bar{t} + \sqrt{2\tau}\mu\Delta\widetilde{W}_{\mathrm{trans},t,j},\\
\Delta\bar{\psi}_{\mathrm{R}_i} &= -\kappa\mu^2\zeta^2\bar{g}_R(\bar{\psi}_{\mathrm{R}_i})\Delta\bar{t} + \sqrt{2\tau}\mu\zeta\Delta\widetilde{W}_{\mathrm{rot},t,i},\\
\Delta\bar{\psi}_{\mathrm{L}_j} &= -\kappa\mu^2\zeta^2\bar{g}_L(\bar{\psi}_{\mathrm{L}_j})\Delta\bar{t} + \sqrt{2\tau}\mu\zeta\Delta\widetilde{W}_{\mathrm{rot},t,j},
\end{aligned}$$

$1 \leq i \leq r, 1 \leq j \leq s$, cf. [9]. The stochastic terms $\Delta\widetilde{W}_{\mathrm{trans},t,i}$, $\Delta\widetilde{W}_{\mathrm{trans},t,j}$, $\Delta\widetilde{W}_{\mathrm{rot},t,i}$ and $\Delta\widetilde{W}_{\mathrm{rot},t,j}$ are $\mathcal{N}(0,\Delta t)$-distributed and can be written as $\Delta\widetilde{W}_{\cdot,t} = Z\cdot\sqrt{\Delta t}$ with $Z \sim \mathcal{N}(0,1)$. For the numerical simulation we choose the following parameter setting:

$$\begin{aligned}
&\eta = 0.1\,\tfrac{\mathrm{Ns}}{\mathrm{m}^2}, && R = 3\,\mathrm{nm}, && \tau = 1\,\mathrm{s}, && L = 10\,\mu\mathrm{m},\\
&k_BT = 5\cdot 10^{-21}\,\mathrm{J}, && \gamma_{\mathrm{rot}} = 8\pi\eta R^2, && \kappa = 10^4, && \Delta\bar{t} = 10^{-9}.
\end{aligned}$$

The formula for the coefficient γ_{rot} is taken from [13] and is adapted to our model. The exponent in the Lennard-Jones potential is chosen to be $n = 6$. The Euler-Maruyama approximation [9] was implemented in C using the linked-cell method [2] for acceleration.

6 Ligand-Receptor Cluster Visualization

Different visualization techniques are used to support the user analyzing the output of the simulation. The major challenge is to cover several orders of magnitude in one data set. The simulation domain is at micrometer scale, both receptors and ligands are only a few nanometers in size, and their movement is at picometer scale depending on the time scale. The visualization allows for a global dynamic, distance-dependent scaling and an additional user-defined scaling of receptors and ligands. When the whole data set is analyzed, up-scaling can be employed to give an overview on the cluster and particle distribution. On the other hand, down-scaling can be used when studying connections or interactions between single particles. Additionally, we provide means for navigation and camera manipulation, like zoom or dolly.

The data from the simulation is processed before the visualization step. Connected components, each component representing a cluster of receptors and ligands, are determined by depth-first search. A unique id is assigned to each cluster and the connectivity is stored explicitly. Using this information, we are able to visualize the ligand-receptor clustering with glyphs as described in the following. Coloring and layered visualizations are used for a better understanding of the data.

6.1 Glyphs

Receptors as well as ligands are assembled of a sphere and multiple cylinders. The combined glyphs for a TNFR1-Fas receptor and a TNF ligand are depicted in Figure 3. The complex protein structure is simplified by enclosing the whole protein with a representative sphere. Binding sites are illustrated by cylinders and can be divided into two classes.

Unbound binding sites: Non-saturated colors indicate free binding sites. The individual sites are modeled with short cylinders sticking out of the particle sphere. The number and the placement, i.e. the rotational angle, are both defined by the particle type. As mentioned before, receptors have two distinct binding sites, colored in red and blue, and ligands have three identical binding sites, colored red. For valid connections the colors must match.

Bound binding sites: The same coloring with increased saturation is applied to binding sites which are bound, i.e. interconnected. A cylinder directly connects the centers of the two particles, since they might not be properly aligned. This is due to the fact, that the underlying model allows connections within a certain domain. This domain can be thought of as sector of a disc centered on the molecule (see Figure 3). In this paper, the apex angle was chosen to be 120 degrees for receptors and 120 degrees for ligands.

Figure 4 shows the general structure of receptors connected to ligands combined with both free and bound binding sites. The connectivity is conveyed by the cylinders of the bound sites and by color. Additional information on a particle is provided in tool tips. This includes the particle id, the ids of bound partners, and among others the size of the cluster where this particle is located in.

In geometry-based approaches several hundreds of vertices are necessary to yield smooth surfaces of spheres and cylinders. Glyphs require only a few coordinates and vectors to describe implicit surfaces. These implicit surfaces are then evaluated during the rendering stage, eliminating most of the expensive geometry transfer to the GPU. In this paper, the visualization employs small glyphs based on [8, 12]. We separate the rendering of cylinders and spheres for more flexibility in our framework. Spheres are simply rendered as a quadrilateral point. The point size is determined in the vertex shader by considering perspective projection and the sphere radius, given in the fourth component of the point coordinates. In the fragment shader, the sphere surface is evaluated and illuminated accordingly. Cylinders are handled in the same way. Additional to the first point describing the cylinder's center point and its radius, the direction and length are transferred to the GPU as vertex attributes. Again, the implicit surface is evaluated in the fragment shader. Silhouette generation with the geometry shader instead of point rendering was neglected because in our scenario the cylinders usually are small and the geometry shader does not give a sufficient speed-up compared to a quadrilateral point rendering [3].

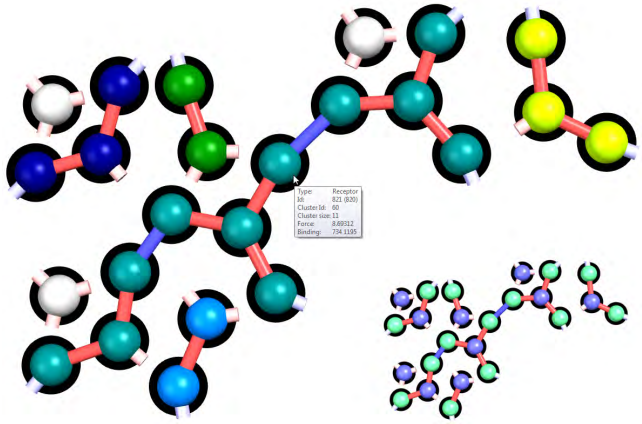

Figure 4: Compounds built from receptors and ligands. Connected binding sites are indicated with high color saturation. Unbound binding sites are rendered light-colored. Coloring according to clusters separates the structure into several cluster. Additional particle information is shown in tool tips. The components of the clusters, ligands and receptors, are shown on the lower right.

In time-dependent data sets, cylindrical glyphs are also used for particle trajectories. The trajectories are shown for user-selected particles to study the motion dynamics.

6.2 Coloring

Color schemes are used to encode local particle information or more global information on the clusters build of the particle. Receptors and ligands are colored according to different properties:

Type: User-defined colors are assigned to each particle type. In this paper, green was chosen for receptors and light blue for ligands (Figure 5(a)).

Cluster: The same color is assigned to all particles of the same cluster. For each cluster the color is picked randomly from a number of predefined colors. This allows to identify regions of connected molecules (Figure 4). However, if the total number of clusters is too high and the cluster are all relatively small, the resulting visualization is cluttered as can be seen in Figure 5(b).

Cluster size: The maximum cluster size of each time step is determined during preprocessing. The size of each cluster is normalized and used for linear interpolation between two colors. The obtained color is then assigned to all molecules which are part of the individual clusters. The user can define a lower and upper limit of the cluster size and outliers can optionally be shown in separate colors. In Figure 5(c), the use of this color scheme reveals several clusters with a size greater than five.

Force: Particles are individually colored according to the magnitude of the applied force. Like in cluster size coloring, two colors are linearly interpolated by the force magnitude. The results (Figure 5(d)) are similar to cluster size coloring because forces, given by the Lennard-Jones potential, directly indicate interacting particles. However, coloring with force magnitude is an important tool

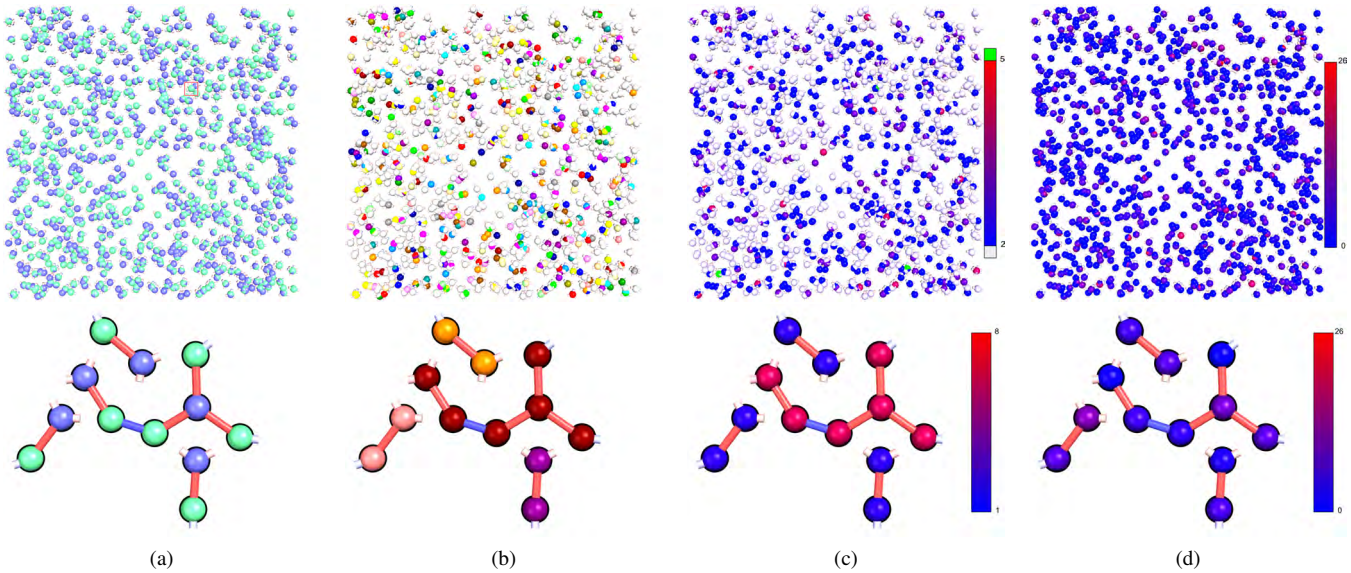

(a) (b) (c) (d)

Figure 5: Different coloring modes. Particles are colored according to particle type, cluster, cluster size, and force (from left to right, close-ups from the highlighted area). Individual clusters with more than one particle are clearly distinguishable with cluster size or force coloring. Clamping was used for cluster size coloring to highlight clusters consisting of more than five particles (green) and make single particles less prominent (light blue). In the first row, the particles are slightly enlarged to be visible.

to identify non-correct bindings between receptors and ligands (see Section 7).

6.3 Dynamic Scaling and Layered Visualization

As aforementioned, the visualization has to deal with different orders of magnitude. Even when looking at a close-up of a few scale-down particles, the differences in size might still matter. Connections between two particles can be hidden by the particles itself since they can intersect each other due to the Lennard-Jones potential. Particle trajectories might be completely or partly occluded by the particle when the movement is very small compared to the particle size. To overcome these issues, we introduce dynamic scaling and a layered visualization.

Dynamic scaling:

The particle radii used in the simulation have to be scaled to allow for a meaningful data analysis. A scaling factor greater than one provides a good overview when looking at the whole simulation domain, but on molecular level particles interpenetrate each other and connections are hidden. In order to unveil the connections, the scaling has to be reduced about one or two orders of magnitude. To support the user during exploration, we provide a dynamic scaling of the radii which is dependent on the camera distance. The user defines a minimum and maximum scaling for both, receptors and ligands. The individual scaling factor of each particle is determined by the squared distance between its position and the camera and is limited by the two extrema. In Figure 7(a), the particles at their original size (scaling factor one) are hardly observable. However, if dynamic scaling is used within the interval $[0.05, 2]$, the data set can be explored without additional adjustment of the radii (Figure 7(b)-(d)).

Layered visualization: Since our data is only two-dimensional, we can make use of the third dimension to reduce occlusion and to emphasize certain aspects like e.g. cluster connections. The different visualization layers are staggered in the third dimension by a user-adjustable offset. A zero offset will produce the same results as a non-layered rendering.

Each layer represents only a specific part of the visualization combined with a visibility flag. We provide layers with different combinations of trajectories, particles, and binding sites. This gives the user the flexibility to adjust the visualization to his current needs by rearranging and switching on the different layers. Figure 6 illustrates the utilization of two layers. The main layer with receptors, ligands, and unbound binding sites and in the upper layer only the particle connections highlighting linked components. In the second example (Figure 9), the trajectories are in a separate layer. Otherwise, the trajectory of the single ligand on the lower left would be completely enclosed by the ligand.

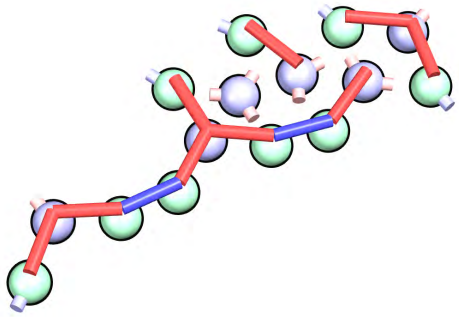

Figure 6: The layered visualization allows to emphasize parts by elevating them in z direction. Here, the connections between receptors and ligands (red) and between two receptors (blue) are highlighted.

7 Results

The simulation parameters were chosen as described in Section 5. We simulated approx. 500 million time steps with $\Delta\bar{t}$ set to 10^{-9} seconds corresponding to 0.5 seconds of simulation time. Every 100,000th step was stored for the subsequent visualization. The length of the simulation domain was set to $1\,\mu$m in both x and y direction with periodic boundary conditions. The number of recep-

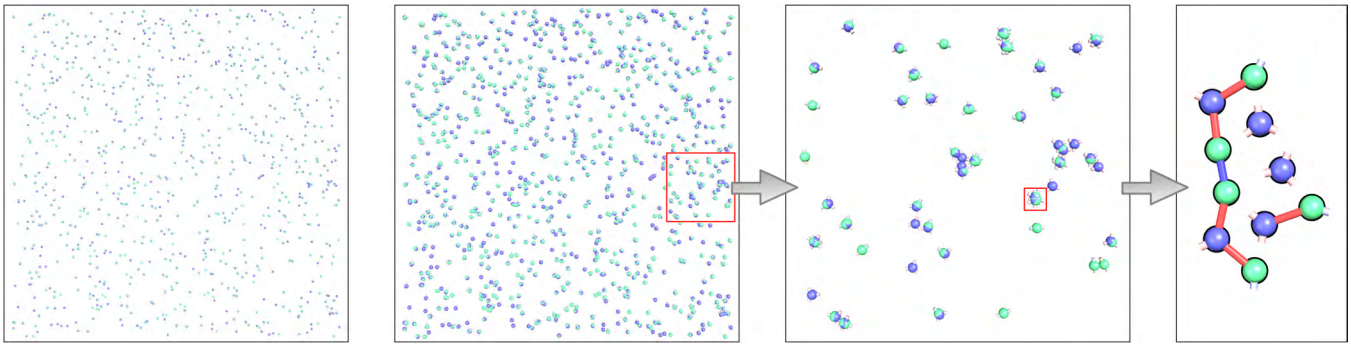

(a) (b) (c) (d)

Figure 7: The dynamic scaling enables the resolution of the structures of ligand-receptor clusters for both, overview and detail views. (a) Particles at the original scale on the whole domain. (b) Dynamic scaling enabled with a scaling factor of two chosen for the domain. (c) Close-up of (b) at dynamic scale one. (d) Zoom-in to cluster-level (dynamic scale 0.05).

tors and ligands was set to 1,000 each. Initial positions and rotations were chosen randomly inside the domain. A non-parallel C implementation of the simulation took 28 days on a Intel Core i7 at 3 GHz and 12 GB RAM.

The visualization is implemented in C++ and OpenGL with GLSL shaders. Glyph data, i.e. positions, radii, and colors, are stored in vertex buffers on the GPU and are updated once per time step. We achieved interactive frame-rates above 100 frames per second on a GeForce 310M with 512 MB RAM.

7.1 User Study on Ligand-Receptor Clustering

Now we present the comments of an informal evaluation by a domain expert. The visualization of the simulation data provides interesting insights into the biological processes for the modeler. Of significant biological interest are the processes involved in apoptosis, especially the extrinsic pro-apoptotic signaling pathway. The external trigger of the extrinsic signaling pathway are ligand-receptor clusters on the cell membrane and the strength of the trigger depends on the size of the clusters. A snap-shot of the particle positions and the binding sites orientation can be displayed and enables the determination of the cluster sizes and the structure of the ligand-receptor clusters. Additionally, the particles can be traced in time. The visualization of the trajectories shows the Brownian motion of the particles and the influence of the attractive and the repulsive interaction between the particles. Furthermore, the visualization of the particle motion enables the estimation of parameter values for the rotation, e.g. the proportional constant κ. Here, the visualization of the receptor and ligand rotation and the emphasizing of the occupied binding sites are valuable tools.

7.2 Qualitative Results

In our visualization, the color schemes have distinct applications. Apart from the distribution of receptors and ligands they reveal important aspects on the data which otherwise would be difficult to spot.

The distribution appears almost uniform in the beginning, but after approx. 50 milliseconds of simulated time clusters of size six emerge. The maximum cluster size increases in time and the maximum observed clusters size of eleven is reached after about 0.45 seconds.

With a switchover between cluster-size coloring and force magnitude we found some inconsistencies in the simulated data. Figure 8 depicts two close-ups of Figure 5(c) and (d). The particles indicated by arrows show a high affecting force which implies interactions, i.e. building of a cluster, but as can be seen in the left image none of those clusters exist yet. At another point of time, the

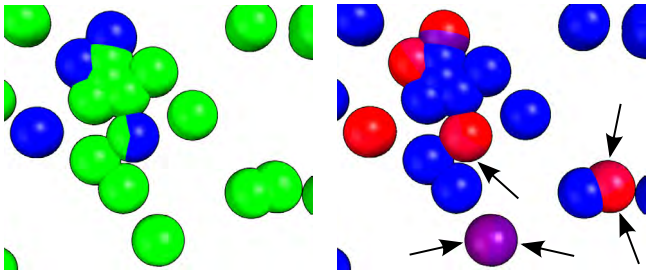

(a) (b)

Figure 8: Switching between cluster-size coloring (a) and force coloring (b) reveals inconsistencies. The arrows indicate particles where the forces imply interactions but clusters are not identified.

force coloring revealed a minor bug in the simulation. Three closeby molecules exhibited a high force, but only two of them were in the same cluster. An inspection showed, that two molecules, a receptor and a ligand, were connected properly but the third one, a second ligand, featured only a connection to the receptor but not vice versa. We figured out, that the first ligand bound to the same receptor where the second ligand was already bound to and overwrote the first connection.

Three ligands and one receptor are tracked over time in Figure 9. Layering reveals the trajectory of the single ligand on the lower left which would otherwise be hidden by the ligand itself because of the small movements. The three parallel trajectories on the top indicate a possible clustering but one receptor cannot bind to two ligands at the same time.

8 Conclusion

The ligand-receptor clustering is an important part of the external stimulus of the extrinsic pro-apoptotic signaling pathway. In this paper, we presented a novel mathematical model for ligand-receptor clustering on the cellular membrane and a glyph-based visualization to analyze the resulting data. Nonlinear coupled stochastic differential equations are employed to simulate a particle system. The particles, representing ligands and receptors, feature explicitly modeled binding sites with which they can interact and build clusters. The mathematical model is flexible concerning the number of particles under consideration, so that the cluster evolution can be studied for different ligand concentrations. The model is restricted to the two-dimensional cell surface and does not take effects like internalization of ligand-receptor clusters into consideration.

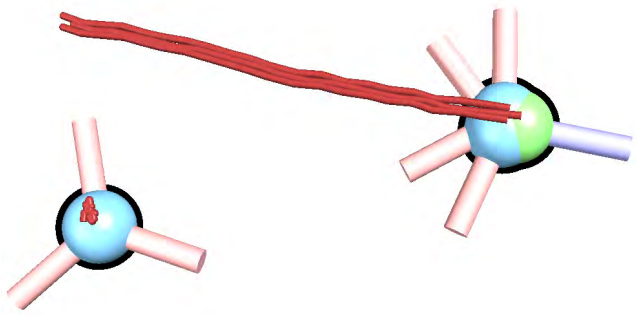

Figure 9: Trajectories of individual particles: a single ligand (bottom left) and one receptor and two ligands (top).

The proposed visualization allows the user to identify such clusters or cluster components. Receptors and ligands as well as their binding sites are rendered as GPU-based glyphs allowing for interactive frame rates on consumer hardware. Color schemes are used to convey different information either on a per-particle basis or on the clusters. The visualization was specifically developed to understand the data and to support the process of model development. It became a helpful tool to detect and fix flaws in the implementation of the simulation. Our domain expert already uses the visualizations for data analysis and model development.

In the future, a major goal is to extend our model of ligand-receptor clustering into three dimensions to simulate the cluster building on the entire cellular membrane. The visualization could e.g. be improved by highlighting invalid bounds. Therefor, it is necessary to perform a more elaborate cluster detection during preprocessing and to flag those invalid bounds. We have also taken first steps into the parallelization of the simulation. Since it is a stochastic process it should map well to the highly parallel architecture of GPUs.

Acknowledgements

The authors would like to thank the German Research Foundation (DFG) for financial support of the project within the Cluster of Excellence in Simulation Technology (EXC 310/1) at the University of Stuttgart.

References

[1] M. Branschädel, A. Aird, A. Zappe, C. Tietz, A. Krippner-Heidenreich, and P. Scheurich. Dual function of cysteine rich domain (crd) 1 of tnf receptor type 1: Conformational stabilization of crd2 and control of receptor responsiveness. *Cellular Signalling*, 22(3):404–414, 2010.

[2] M. Griebel, S. Knapek, and G. Zumbusch. *Numerical simulation in molecular dynamics*. Springer, 2007.

[3] S. Grottel, G. Reina, and T. Ertl. Optimized data transfer for time-dependent, gpu-based glyphs. In *IEEE Pacific Visualization Symposium (PacificVis '09)*, pages 65–72, 2009.

[4] S. Grottel, G. Reina, J. Vrabec, and T. Ertl. Visual verification and analysis of cluster detection for molecular dynamics. In *IEEE Visualization 2007*, pages 1624–1631, 2007.

[5] S. Gumhold. Splatting illuminated ellipsoids with depth correction. In *International Fall Workshop on Vision, Modelling and Visualization*, pages 245–252, 2003.

[6] C. Guo and H. Levine. A thermodynamic model for receptor clustering. *Biophysical Journal*, 77(5):2358–2365, 1999.

[7] M. A. Haidekker, T. Ling, M. Anglo, H. Y. Stevens, J. A. Frangos, and E. A. Theodorakis. New fluorescent probes for the measurement of cell membrane viscosity. *Chemistry & Biology*, 8(2):123–131, 2001.

[8] T. Klein and T. Ertl. Illustrating magnetic field lines using a discrete particle model. In *Vision, Modelling and Visualization (VMV '04)*, pages 387–394, 2004.

[9] P. E. Kloeden and E. Platen. *Numerical solution of stochastic differential equations*. Stochastic Modelling and Applied Probability. Springer, 1992.

[10] C. Müller, S. Grottel, and T. Ertl. Image-space GPU metaballs for time-dependent particle data sets. In *Vision, Modelling and Visualization (VMV '07)*, pages 31–40, 2007.

[11] A. S. Perelson and C. DeLisi. Receptor clustering on a cell surface. I. Theory of receptor cross-linking by ligands bearing two chemically identical functional groups. *Mathematical Biosciences*, 48(1-2):71–110, 1980.

[12] G. Reina and T. Ertl. Hardware-accelerated glyphs for mono-and dipoles in molecular dynamics visualization. In *Eurographics/IEEE VGTC Symposium on Visualization*, pages 177–182, 2005.

[13] P. Saffman and M. Delbrück. Brownian motion in biological membranes. *National Academy of Sciences of the United States of America*, 72(8):3111–3113, 1975.